

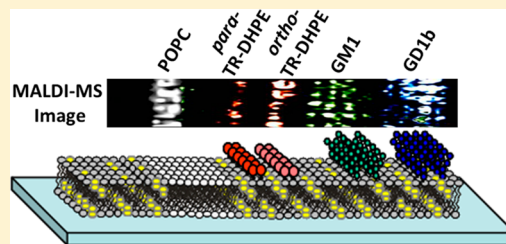
# Coupling Supported Lipid Bilayer Electrophoresis with Matrix-Assisted Laser Desorption/Ionization-Mass Spectrometry Imaging

Hudson P. Pace, Stacy D. Sherrod, Christopher F. Monson, David H. Russell, and Paul S. Cremer\*

Department of Chemistry, Texas A&M University, College Station, Texas 77843, United States

**S** Supporting Information

**ABSTRACT:** Herein, we describe a new analytical platform utilizing advances in heterogeneous supported lipid bilayer (SLB) electrophoresis and matrix-assisted laser desorption/ionization-mass spectrometry (MALDI-MS) imaging. This platform allowed for the separation and visualization of both charged and neutral lipid membrane components without the need for extrinsic labels. A heterogeneous SLB was created using vesicles containing monosialoganglioside GM1, disialoganglioside GD1b, POPC, as well as the ortho and para isomers of Texas Red-DHPE. These components were then separated electrophoretically into five resolved bands. This represents the most complex separation by SLB electrophoresis performed to date. The SLB samples were flash frozen in liquid ethane and dried under vacuum before imaging with MALDI-MS. Fluorescence microscopy was employed to confirm the position of the Texas Red labeled lipids, which agreed well with the MALDI-MS imaging results. These results clearly demonstrate this platform's ability to isolate and identify nonlabeled membrane components within an SLB.



Supported lipid bilayer (SLB) systems have emerged as an important platform for creating models of phospholipid membranes, as well as for studying the interactions and structure of various membrane components.<sup>1–4</sup> With the use of this platform, systems that allow for the manipulation of membrane components within the plane of the bilayer have been investigated by many research groups.<sup>5–12</sup> Most of these advances are being driven by a desire to develop methods to separate or concentrate membrane components. To this end, our group has demonstrated the ability to separate multiple species bearing the same charge by introducing a heterogeneous SLB system.<sup>13</sup> In these systems, analyte-containing SLBs were patterned into a separation SLB, whose composition was tuned to optimize separation conditions. Advancements in cushioning architectures have increased the mobile fraction of transmembrane proteins embedded in SLBs.<sup>14–16</sup> Additionally, our group recently demonstrated the importance of maintaining strict control over the buffering environment of SLBs during electrophoresis, particularly for proteins, and developed the required technology.<sup>17,18</sup> Each of these accomplishments is critical for developing a method capable of separating and studying membrane proteins within their native environment (i.e., the phospholipid bilayer).

Separations in lipid bilayers have traditionally been monitored by fluorescence microscopy.<sup>5,6,13,17,18</sup> Light-based optical imaging is an effective analytical tool for measuring the mobility of membrane-bound species in the plane of the bilayer in real-time; however, the use of extrinsic molecular tags (e.g., fluorophores) imposes limitations and possible complications on the experiments.<sup>19</sup> The conjugation of a fluorophore to an analyte can affect the analyte's mobility in the bilayer by altering both its size and net charge.<sup>17,18</sup> Additionally, conjugation may occur at a site that may inhibit interactions between analytes.

Lastly, there are only a finite number of fluorescent tags that can be employed within a single system without spectral overlap, which ultimately leads to a limitation on the number of different species that can be detected in a single sample.

A technique that has shown promise for spatially resolving and characterizing membrane species is imaging mass spectrometry (MS).<sup>20–22</sup> Imaging MS is inherently a label-free method, due to the use of an analyte's mass to charge ratio ( $m/z$ ) for detection. While secondary ion MS (SIMS) is capable of imaging many components of SLBs,<sup>23</sup> it suffers from a narrow mass range, typically less than 1 kDa, and a high degree of analyte fragmentation.<sup>24</sup> Matrix-assisted laser desorption ionization (MALDI)-MS has been utilized to image complex biological samples (e.g., tissue specimens). MALDI-MS has the ability to produce large intact singly charged molecular ions. These ions generate deconvoluted spectra, which allows for ease of analyte identification.<sup>22</sup> While imaging MALDI-MS does not have the spatial resolution of SIMS, it is more than adequate for resolving the bands of the separated bilayer species described below. Additionally, the relatively large imaging area required for these separation studies ( $\sim 3 \text{ mm} \times 1 \text{ cm}$ ) exceeds the practical sampling area for SIMS but can be accomplished by MALDI-MS imaging. The use of analyte prefractionation from complex biological mixtures prior to MS analysis is often required to prevent ion suppression effects.<sup>25</sup> SLB electrophoresis shows promise at being able to fulfill this role for membrane components. As such, MALDI-MS imaging could potentially

Received: March 25, 2013

Accepted: May 14, 2013

Published: June 3, 2013





**Figure 1.** An illustration of the separation of five membrane components using heterogeneous SLB electrophoresis. The four negatively charged components, GD1b (blue), GM1 (green), ortho-TR-DHPE (pink) and para-TR-DHPE (red) were separated from a neutral lipid, POPC (white), which marked the origin. The use of cholesterol (yellow) in the separation matrix allows for the separation of this complex mixture. The location of each of the species was found by MALDI-MS imaging.

map the location of hundreds of membrane components in SLBs after separation.

Herein, we report the separation of a five-component mixture of membrane-bound species performed by SLB electrophoresis. Additionally, this is the first separation of two naturally occurring cell surface receptors using SLB electrophoresis. The lipid receptors, monosialoganglioside GM1 and disialoganglioside GD1b, play several important physiological roles and have been implicated in disease pathways via cell-pathogen docking.<sup>26–28</sup> In these experiments, the ortho and para isomers of Texas Red 1,2-dihexadecanoyl-*sn*-glycero-3-phosphoethanolamine (TR-DHPE), two fluorophore-labeled lipids, provided an *in situ* means to monitor the electrophoretic separation process via fluorescence microscopy. MALDI-MS imaging was utilized *ex situ* to create an ion map of the SLB that revealed the location of each membrane species after the separation was completed. Figure 1 is a schematic illustration of the heterogeneous SLB electrophoretic separation studied in this report.

## EXPERIMENTAL SECTION

**Preparation of Glass Substrates.** Corning coverslips (no. 1 1/2, 24 × 40 mm) were boiled in a 1:7 diluted 7× detergent (MP Biomedicals, Solon, OH) in water, thoroughly rinsed with 18 MΩ water, blown dry with compressed nitrogen, and then annealed at 530 °C for 5 h. These substrates were stored in a clean manufacturer's container and used within two weeks.

**Preparation of Vesicles.** Small unilamellar vesicles (SUVs) were prepared using the freeze–thaw/extrusion method.<sup>29,30</sup> Briefly, lipids dissolved in chloroform (or methanol:chloroform, 1:2, for gangliosides) were mixed in the desired mole ratios and the organic solvent was evaporated under a stream of nitrogen followed by complete solvent removal under vacuum overnight. The two vesicle compositions used in these experiments were (i) 25 mol % cholesterol, 37.5 mol % 1,2-dilauroyl-*sn*-glycero-3-phosphocholine (DLPC), 37.5 mol % 1,2-dieicosenoyl-*sn*-glycero-3-phosphocholine (DEPC), and (ii) 10 mol % GD1b, 3 mol % GM1, 2 mol % TR-DHPE, and 85 mol % 1-palmitoyl-2-oleoyl-*sn*-glycero-3-phosphocholine (POPC). Desiccated lipid mixtures were rehydrated in PBS (10 mM sodium phosphate buffer and 150 mM NaCl, pH 7.5) and subjected to 10 freeze/thaw cycles using liquid nitrogen and warm water. The vesicle solutions were extruded 10 times through a polycarbonate filter containing 100 nm pores (Whatman, Florham Park, NJ), diluted to 1 mg/mL with pure water, and stored at 4 °C until use. Vesicles were found to have a sharp distribution around 100 nm by dynamic light scattering measurements (90Plus Particle Size Analyzer, Brookhaven Instrument Corp., Holtsville, NY).

**Preparation of PDMS Wells and Stamps.** Polydimethylsiloxane (PDMS) was used to create wells for containing the SLBs. Sheets of uniform thickness (150 ± 15 μm) were created by polymerizing the PDMS between two annealed/silanized

glass slides using the previously described glass coverslips as spacers. The glass slides were silanized by the evaporative coating of hexamethyldisilazane (HMDS). These sheets were cut to the dimensions of the glass coverslips and a channel of ~22 mm by 4 mm was cut into their center. These wells were cleaned and applied to the glass substrate. Bubbles between the PDMS wells and glass were removed via mechanical pressure. PDMS stamps were created in a similar fashion, but the polymer films were ~2 mm thick. The stamps were cut to have a foot print of ~3 mm by ~600 μm. They were then rinsed with purified water and ethanol, blown dry with nitrogen, oxygen plasma cleaned for 1 min bottom-side-up, and finally placed in the desired location on the glass substrate within the PDMS well.

**Preparation of Heterogeneous Supported Lipid Bilayers.** Once the PDMS well and stamp were positioned on the coverslip, 50 μL of the primary vesicle solution, (i), was used to create the separation SLB (Figure 2A). After 5 min, the well was thoroughly rinsed and the stamp removed. Next, 20

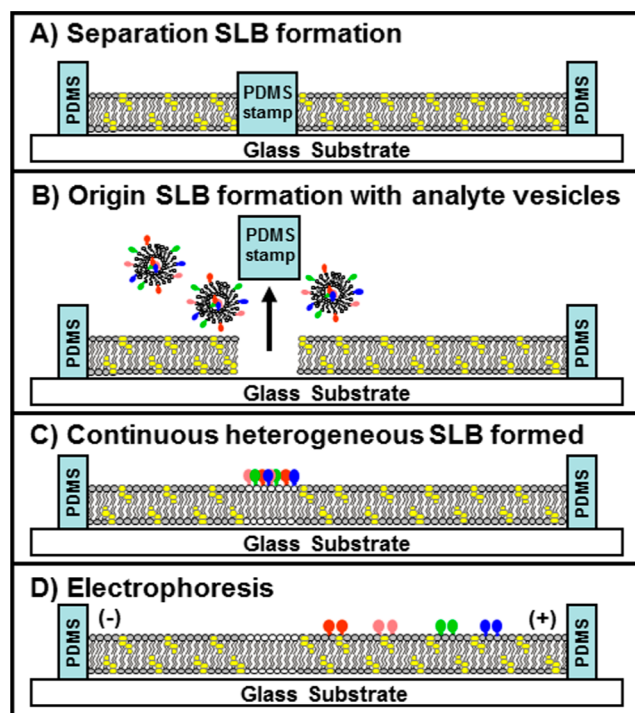


**Figure 2.** Schematic representation of the stamping method employed for heterogeneous SLB preparation. (A) The separation SLB was formed in the PDMS well with the PDMS stamp in place. (B) After rinsing, the PDMS stamp was removed and the analyte vesicle solution was added. (C) After rinsing away excess/unfused vesicles, a well-defined continuous heterogeneous SLB remained. (D) During electrophoresis, charged analytes (lipids, etc.) migrated into the separation region from the origin.

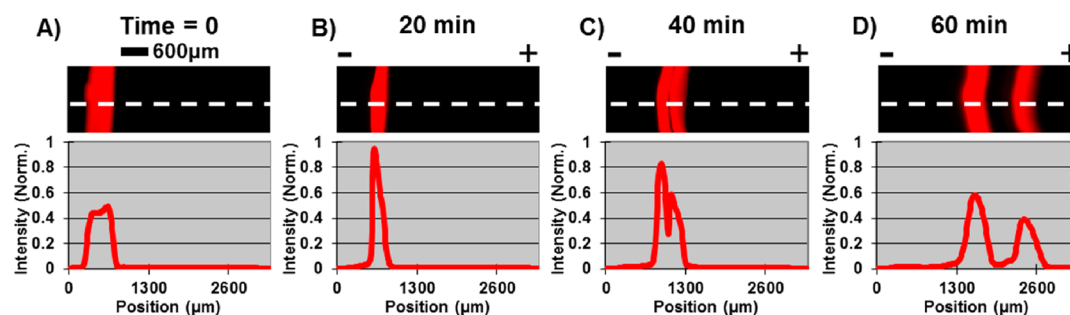


**Figure 3.** (A–D) Fluorescent images (via TR-DHPE) and line scans showing the progression of analyte separation during electrophoresis. The line scans illustrate that the analyte band narrowed and increased in intensity (concentration) at the perimeter of the origin SLB before proceeding into the separation region.

$\mu\text{L}$  of a second vesicle solution, (ii), was introduced along with 20  $\mu\text{L}$  of 4 M NaCl (Figure 2B). It should be noted that such high ionic strength screened the repulsion between the negatively charged analyte vesicles and the negatively charged substrate, facilitating the vesicle fusion process.<sup>31</sup> These vesicles fused to the areas previously occupied by the PDMS stamp and made a continuous bilayer with the separation SLB. This vesicle solution was allowed to incubate for 5 min before thoroughly rinsing with purified water. The process created a discrete secondary SLB (the origin, in the previous location of the PDMS stamp) inside a larger primary SLB (separation region), as illustrated in Figure 2C. The charged analyte material could then be separated by electrophoresis (Figure 2D). All samples described herein were prepared in this manner and with the vesicle compositions described above.

To separate membrane components, a line of the analyte-containing bilayer was patterned into a separation bilayer as described in Figure 2. Such heterogeneously patterned lipid mixtures allow for simple one-dimensional separations of the analyte material normal to the direction of the analyte strip.<sup>7</sup> Previously, heterogeneous SLBs were often constructed using a “scratch and backfill” method rather than the new PDMS stamp-blocking technique employed herein. The older method generated  $\sim 100\ \mu\text{m}$  wide analyte-containing origin regions. Such a method can be disadvantageous if scratches are also made in the underlying solid support during the removal of the SLB material. Moreover, the width of such analyte lines is often difficult to control by scratching. In the current context, the width needs to be greater to accommodate the laser spot size of the MALDI-MS instrument. Thus, PDMS stamps were employed to create a heterogeneous SLB system with an approximately  $600\ \mu\text{m}$  wide analyte strip. This wider line width allows for a greater amount of analyte material to be deposited and separated. It also provides a sharper interface between the two chemically distinct SLB regions.

**Supported Lipid Bilayer Electrophoresis.** The heterogeneous SLB was coupled to an electrophoretic flow cell device, described previously.<sup>17</sup> This Teflon device, which had two buffer channels on each side of the observation region of the supported bilayer, allowed electrophoresis to occur under constant buffering conditions while removing the products of electrolysis. The outer two channels contained platinum electrodes, while the inner channels helped isolate the observation region of the supported bilayer from the electrodes. Continuous buffer flow through all four channels mitigated Joule heating and ensured the pH remained uniform within the observation region. The experiments reported below were performed under a constant flow of 1 mM phosphate buffer

(no NaCl, pH 7.8,  $\sim 1.5\ \text{mL/min}$  flow rate) for 1 h at 600 V (333 V/cm, average current  $\sim 35\ \mu\text{A}$ ). The drain solutions from each channel were monitored by a pH meter. No measurable pH variations were observed for the inner channels of the device under these conditions. This is consistent with the idea that no pH variations occurred within the observation region. Electrophoretic separation of the ortho and para isomers of TR-DHPE was monitored in real time, using a Nikon Eclipse 80i upright epifluorescence microscope equipped with a Micro-MAX 1024 CCD camera (Princeton Instruments) and a  $4\times$  objective.

**Supported Lipid Bilayer Preparation for MALDI-MS Imaging.** A comprehensive description of the protocol used for preparing an SLB for MALDI-MS imaging can be found in the supporting material. Briefly, after electrophoretic separation, the flow cell was deconstructed under water. The sample was flash-frozen in liquid ethane that was cooled by liquid  $\text{N}_2$ . It was then freeze-dried using a prechilled desiccator contained in a box freezer under vacuum. The sample’s integrity was checked using fluorescence microscopy. MALDI matrix was uniformly applied to the sample with an airbrush. This matrix consisted of 10 mg/mL  $\alpha$ -cyano-4-hydroxycinnamic acid, 30 mg/mL 2,5-dihydroxybenzoic acid, and 20 mM diammonium citrate in 10 mL of 2:1:0.03 acetone:methanol:water. After matrix application, the sample was mounted on a clean MALDI plate using two-sided copper tape. After removal of the PDMS well, a clean nickel grid (70 lines per inch) was placed over the sample and secured in place using single-sided copper tape.

**Imaging Mass Spectrometry.** Bilayer samples were analyzed using a 4700 Proteomics Analyzer MALDI TOF/TOF (Applied Biosystems, Foster City, CA) mass spectrometer under optimized conditions in the reflection mode. The mass spectra were externally calibrated using standards spotted on a mounted glass substrate. The laser spot size was an ellipse with dimensions of  $80 \times 100\ \mu\text{m}$ . This spot was rastered over the sample with a step size of  $80\ \mu\text{m}$  along a row and  $100\ \mu\text{m}$  between each row by using 4700 Imaging software (Novartis and Applied Biosystems). Individual mass spectra represented the average of 250 laser shots, and BioMap software (Novartis, Basel, Switzerland) was used to generate ion-specific maps of the sample. Mass assignments were validated by comparison to the spectra taken from pure reagents.

## RESULTS AND DISCUSSION

**Heterogeneous SLB Electrophoresis.** Supported analyte bilayers with 2 mol % TR-DHPE were employed to discern the initial quality of the patterned SLB and the progression of the electrophoretic process. Fluorescence micrographs illustrating



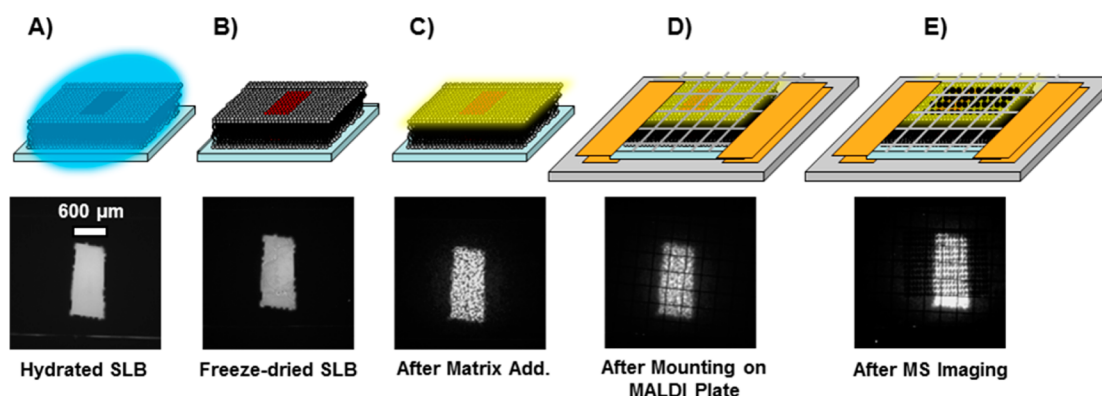


**Figure 4.** A diagram of the steps in the sample preparation process used to prepare SLBs for MALDI-MS imaging. The (A) hydrated lipid bilayer was (B) freeze-dried and prepared for MS analysis by (C) matrix application and (D) mounted onto a MALDI plate with a Ni grid using Cu tape. (E) After MS imaging, the array of black dots indicates the raster pattern of the laser. Below each illustration is a corresponding fluorescence image (via TR-DHPE).

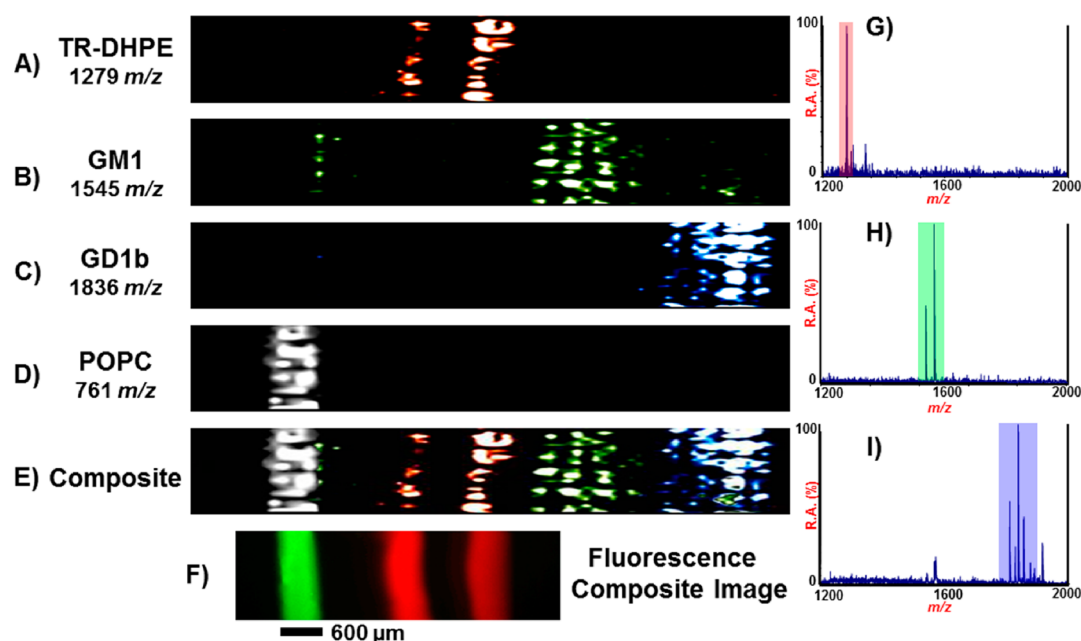


**Figure 5.** MALDI-MS imaging of a heterogeneous SLB post electrophoresis. (A–D) Ion-specific images of the SLB components: (A) TR-DHPE, (B) GM1, (C) GD1b, and (D) POPC. (E) A composite image overlaying the ion-specific images from A–D, illustrating the separation of the five analytes. (F) A composite image of two fluorescence images. The green band represents TR-DHPE and was taken prior to electrophoresis. The red bands are the two TR-DHPE isomers after SLB electrophoresis. (G–I) Representative mass spectra taken from regions indicated in (A), (B), and (C). The highlighted regions show characteristic ions produced by each analyte: (G) ortho- and para-TR-DHPE ( $m/z$  1279), (H) GM1 ( $m/z$  1545 and 1573), and (I) GD1b ( $m/z$  1818–1886).

the electrophoretic separation of the ortho and para isomers of the fluorescent reporter as a function of time are shown in Figure 3. As can be seen in the image, the initial  $\sim 600\ \mu\text{m}$  analyte strip (Figure 3a) was narrowed to  $\sim 200\ \mu\text{m}$  after  $\sim 20$  min (Figure 3b). This narrowing was a direct consequence of the decrease in the mobility of the fluorophores in the separation bilayer compared with the analyte bilayer. Indeed, the presence of 25 mol % cholesterol in the former reduces the diffusion constant by a factor of 2.<sup>13</sup> This sharp transition in viscosity at the boundary between the origin and separation regions produces an effect comparable to the use of a stacking layer in gel electrophoresis, which concentrates the contents of the well prior to separation. After 40 min, the two fluorescent isomers moved completely into the separation region and began to resolve (Figure 3c). Moreover, the lines remained

thinner than the origin ( $\sim 400\ \mu\text{m}$  wide) band. Although some band broadening did occur with time, near baseline separation was achieved after 60 min (Figure 3d). What is not observed in these micrographs is the concomitant separation of the other three analyte components which were also present: GM1, GD1b, and POPC. Indeed, these species lacked fluorescent tags.

**SLB Preparation for MS Imaging.** MALDI-MS imaging researchers have explored various methods of freezing samples, mounting them on MALDI plates, and applying the matrix.<sup>32</sup> These procedures require adaptation for our samples, due to the insulating nature of the substrate. The five-step process we have employed is shown schematically with corresponding fluorescent images provided below each illustration (Figure 4). The composition of the heterogeneous SLB in these images is

the same as provided in Figure 3. The only difference is that this bilayer was not subjected to electrophoresis.

In the first step, a heterogeneous SLB was formed (Figure 4A). Next, the sample had to be removed from its hydrated environment and made vacuum compatible without causing significant analyte delocalization. To do this, the membrane was flash frozen by immersion in liquid ethane and then freeze-dried under vacuum at  $-20\text{ }^{\circ}\text{C}$ . After this, the dried lipid film was returned to room temperature and ambient conditions (Figure 4B). It should be noted that the freeze-drying process disrupted the local structure of the SLB, probably by having the alkyl tails of the lipids reorient to face the air. Nevertheless, the general two-dimensional microscale arrangement of the lipid material remained unchanged. The dried lipid film was then coated with MALDI matrix via air brushing (Figure 4C). The sample was then mounted to a MALDI plate by conductive Cu tape with the glass substrate sandwiched between a Ni grid and the plate (Figure 4D). The conductive copper tape and Ni grid were necessary to prevent charge build up from the formation of ions on the insulating glass substrate during MALDI imaging. Finally, a square array of dark spots could be seen in the fluorescent images after the surface was subjected to laser ablation during the MALDI imaging process (Figure 4E).

#### MALDI-MS Imaging of the SLB after Electrophoresis.

Imaging MALDI-MS was used to map the position of each component in the SLB after electrophoresis (Figure 5). The samples imaged herein consisted of five analyte components: TR-DHPE ortho and para isomers, GM1, GD1b, and POPC. Figure 5 (panels A–D) shows individual ion-specific images of the five separated analyte components: the ortho- and para-TR-DHPE isomers ( $m/z$  1279, corresponding to  $[\text{TR-DHPE}(16:0/16:0) - \text{H}]^{-}$ ), GM1 ( $m/z$  1573, corresponding to  $[\text{GM1}(20:0/d18:1) - \text{H}]^{-}$ ), GD1b ( $m/z$  1836, corresponding to  $[\text{GD1b}(18:0/d18:1) - \text{H}]^{-}$ ), and POPC ( $m/z$  761, corresponding to  $[\text{POPC} + \text{H}]^{+}$ ). There are two bands present in Figure 5A because the TR-DHPE isomers separated from each other during electrophoresis as also shown in Figure 3. On the other hand, the appearance of the more closely spaced horizontal and vertical stripes in the individual bands in Figure 5 (panels A–D) is due to the presence of the Ni grid placed over the sample. This prevented ionization from the surface within the grid's shadow. A composite image of the four ion-specific images is shown in Figure 5E. As can be seen, the five components are well-separated from each other and easily identified chemically by their mass-to-charge ratio.

Figure 5F is a composite of the false color fluorescent images taken of the identical supported bilayer sample before freeze-drying. The green fluorescent band designates the location of the two TR-DHPE isomers before the electrophoresis process was begun. This band essentially marks the origin for the analyte mixture that was separated. The red bands represent these same TR-DHPE isomers after electrophoresis for 1 h at 333 V/cm. As can be seen, the MS imaging location of POPC (white band) and origin position of the TR-DHPE isomers (green band) match up very well. The 761  $m/z$  (white) band from the MALDI imaging is, however, modestly broader, which should represent the diffusion of POPC which occurred during the 60 min electrophoresis process. Also, the position of the TR-DHPE bands from fluorescent imaging after electrophoresis match the positions of the two bands found at 1279  $m/z$  from MALDI-MS imaging. This represents excellent confirmation that the MALDI-MS imaging procedure for supported bilayers developed herein can indeed be used to ascertain the position

of nonlabeled membrane components after separation within an SLB.

The mass spectra in Figure 5 (panels G–I) highlight the specific masses used to produce the ion-specific images in Figure 5 (panels A–C), respectively. As can be seen, each mass spectrum has several highlighted peaks that correspond to specific chemical species characteristic of that lipid analyte. The peak assignments are further described in the Supporting Information. The most abundant of these specific characteristic ions was chosen in each case to generate the ion-specific images shown in Figure 5 (panels A–C). It should be noted that ions present at  $m/z$  1545 and 1573 in Figure 5I result from the loss of sialic acid (291 Da) from GD1b ( $m/z$  1836 and 1864, respectively) and have been observed previously.<sup>33</sup> It should also be noted that the mass spectra shown in Figure 5 (panels G–I) were specifically acquired from the respective high-abundance regions for each individual analyte.

In these experiments, POPC was employed to mark the location of the origin (Figure 5d) because it exhibited no electrophoretic motion during the separation due to its net neutral charge under the experimental buffering conditions (pH 7.8). The TR-DHPE isomers and gangliosides migrated out of the origin toward the anode due to their net negative charges under these conditions. The singly charged TR-DHPE isomers, however, migrate significantly slower than GM1, which also carried a single negative charge. The net migration of each bilayer species is the result of both electrophoretic and electroosmotic forces. Molecular dynamics simulations have demonstrated that the TR-DHPE's headgroup spends most of its time located in the hydrophobic (highly viscous) region of the bilayer.<sup>34</sup> By contrast, gangliosides have hydrophilic polysaccharide head groups that have minimal interaction with the bilayer's hydrophobic core.<sup>35</sup> Thus, it appears that the greater interactions of the Texas Red headgroup with the bilayer interior leads to reduced electrophoretic migration. Finally, GD1b and GM1 separate from each other on simple electrostatic grounds, as the former carries a double-negative charge due to the presence of two sialic acids in its headgroup.

The combination of MALDI-MS imaging and SLB electrophoresis offers a unique platform for the separation of membrane components and their complexes within the bilayer environment. The use of separation techniques to prefractionate analytes from complex biological samples prior to MS analysis is a common method for circumventing analyte ion-suppression effects.<sup>25</sup> Indeed, it was observed that GM1 suppressed the ionization of GD1b prior to separation (Supporting Information). Thus, SLB electrophoresis shows great potential for being able to satisfy this role for membrane components. Moreover, this technique could be used in the future to investigate membrane peptide aggregates and clustering as well as lipid–cholesterol interactions and ligand–receptor binding.

## CONCLUSION

This work brought together developments in SLB construction, electrophoresis, and MALDI-MS imaging strategies to provide a new analytical platform for membrane component separation applications. Herein, the capacity to purify two gangliosides from a multicomponent mixture into discrete regions within the bilayer was demonstrated. Additionally, each of the five analytes was mapped using the inherently label-free technique of MS imaging. This technology is currently being adapted in concert with developments in SLB cushioning and inverted

membrane vesicle preparation to create highly mobile SLBs, containing nonreconstituted native membranes for the eventual separation and study of membrane proteins.

## ■ ASSOCIATED CONTENT

### ■ Supporting Information

Additional information as noted in text. This material is available free of charge via the Internet at <http://pubs.acs.org>.

## ■ AUTHOR INFORMATION

### Corresponding Author

\*E-mail: [psc11@psu.edu](mailto:psc11@psu.edu).

### Notes

The authors declare no competing financial interest.

## ■ ACKNOWLEDGMENTS

PSC thanks the National Institutes of Health (Grant GM070622) and DHR thanks the U. S. Department of Energy, Division of Chemical Sciences, BES (Grant DE-FG02-04ER15520) for funding.

## ■ REFERENCES

- (1) Brian, A. A.; McConnell, H. M. *Proc. Natl. Acad. Sci. U.S.A.* **1984**, *81*, 6159.
- (2) Tamm, L. K.; McConnell, H. M. *Biophys. J.* **1985**, *47*, 105.
- (3) Sackmann, E. *Science* **1996**, *271*, 43.
- (4) Castellana, E. T.; Cremer, P. S. *Surf. Sci. Rep.* **2006**, *61*, 429.
- (5) Stelzle, M.; Miehlich, R.; Sackmann, E. *Biophys. J.* **1992**, *63*, 1346.
- (6) Cremer, P. S.; Groves, J. T.; Kung, L. A.; Boxer, S. G. *Langmuir* **1999**, *15*, 3893.
- (7) Suzuki, K.; Hosokawa, K.; Maeda, M. *J. Am. Chem. Soc.* **2008**, *130*, 1542.
- (8) Smith, E. A.; Coym, J. W.; Cowell, S. M.; Tokimoto, T.; Hruby, V. J.; Yamamura, H. I.; Wirth, M. J. *Langmuir* **2005**, *21*, 9644.
- (9) Jönsson, P.; Beech, J. P.; Tegenfeldt, J. O.; Höök, F. *J. Am. Chem. Soc.* **2009**, *131*, 5294.
- (10) Zhang, H.-Y.; Hill, R. J. *Soft Matter* **2010**, *6*, 5625.
- (11) Cheetham, M. R.; Bramble, J. P.; McMillan, D. G. G.; Krzeminski, L.; Han, X.; Johnson, B. R. G.; Bushby, R. J.; Olmsted, P. D.; Jeuken, L. J. C.; Marritt, S. J.; Butt, J. N.; Evans, S. D. *J. Am. Chem. Soc.* **2011**, *133*, 6521.
- (12) Nabika, H.; Oowada, M.; Murakoshi, K. *Phys. Chem. Chem. Phys.* **2011**, *13*, 5561.
- (13) Daniel, S.; Diaz, A. J.; Martinez, K. M.; Bench, B. J.; Albertorio, F.; Cremer, P. S. *J. Am. Chem. Soc.* **2007**, *129*, 8072.
- (14) Goennenwein, S.; Tanaka, M.; Hu, B.; Moroder, L.; Sackmann, E. *Biophys. J.* **2003**, *85*, 646.
- (15) Tanaka, M.; Sackmann, E. *Nature* **2005**, *437*, 656.
- (16) Diaz, A. J.; Albertorio, F.; Daniel, S.; Cremer, P. S. *Langmuir* **2008**, *24*, 6820.
- (17) Monson, C. F.; Pace, H. P.; Liu, C. M.; Cremer, P. S. *Anal. Chem.* **2011**, *83*, 2090.
- (18) Liu, C. M.; Monson, C. F.; Yang, T. L.; Pace, H.; Cremer, P. S. *Anal. Chem.* **2011**, *83*, 7876.
- (19) Burns, A. R. *Langmuir* **2003**, *19*, 8358.
- (20) Chaurand, P.; Caprioli, R. M. *Electrophoresis* **2002**, *23*, 3125.
- (21) Chaurand, P.; Norris, J. L.; Cornett, D. S.; Mobley, J. A.; Caprioli, R. M. *J. Proteome Res.* **2006**, *5*, 2889.
- (22) Heeren, R. M. A.; Smith, D. F.; Stauber, J.; Kukrer-Kaletas, B.; MacAleese, L. *J. Am. Soc. Mass. Spectrom.* **2009**, *20*, 1006.
- (23) Kraft, M. L.; Weber, P. K.; Longo, M. L.; Hutcheon, I. D.; Boxer, S. G. *Science* **2006**, *313*, 1948.
- (24) Heeren, R. M. A.; McDonnell, L. A.; Amstalden, E.; Luxembourg, S. L.; Altelaar, A. F. M.; Piersma, S. R. *Appl. Surf. Sci.* **2006**, *252*, 6827.
- (25) Righetti, P. G.; Castagna, A.; Antonioli, P.; Boschetti, E. *Electrophoresis* **2005**, *26*, 297.
- (26) Singh, A. K.; Harrison, S. H.; Schoeniger, J. S. *Anal. Chem.* **2000**, *72*, 6019.
- (27) Imberty, A.; Varrot, A. *Curr. Opin. Struct. Biol.* **2008**, *18*, 567.
- (28) Lopez, P. H. H.; Schnaar, R. L. *Curr. Opin. Struct. Biol.* **2009**, *19*, 549.
- (29) Hope, M. J.; Bally, M. B.; Webb, G.; Cullis, P. R. *Biochim. Biophys. Acta, Biomembr.* **1985**, *812*, 55.
- (30) Mayer, L. D.; Hope, M. J.; Cullis, P. R. *Biochim. Biophys. Acta, Biomembr.* **1986**, *858*, 161.
- (31) Cremer, P. S.; Boxer, S. G. *J. Phys. Chem. B* **1999**, *103*, 2554.
- (32) Schwartz, S. A.; Reyzer, M. L.; Caprioli, R. M. *J. Mass Spectrom.* **2003**, *38*, 699.
- (33) Zarei, M.; Bindila, L.; Souady, J.; Dreisewerd, K.; Berkenkamp, S.; Muthing, J.; Peter-Katalinic, J. *J. Mass Spectrom.* **2008**, *43*, 716.
- (34) Skaug, M. J.; Longo, M. L.; Faller, R. *J. Phys. Chem. B* **2009**, *113*, 8758.
- (35) Roy, D.; Mukhopadhyay, C. *J. Biomol. Struct. Dyn.* **2002**, *19*, 1121.